

## Detonation Type Ram Accelerator: A Computational Investigation

Sunil Bhat

*Armament Research & Development Establishment, Pune 41 021*

### ABSTRACT

An analytical model explaining the functional characteristics of detonation type ram accelerator is presented. Major flow processes, namely, (i) supersonic flow over the cone of the projectile, (ii) initiation of conical shock wave and its reflection from the tube wall, (iii) supersonic combustion, and (iv) expansion wave and its reflection are modelled. Taylor-Maccoll approach is adopted for modelling the flow over the cone of the projectile. Shock reflection is treated in accordance with wave angle theory for flows over the wedge. Prandtl-Mayer analysis is used to model the expansion wave and its reflection. Steady one-dimensional flow with heat transfer along with Rayleigh line equation for perfect gases is used to model supersonic combustion. A computer code is developed to compute the thrust produced by combustion of gases. Ballistic parameters like thrust-pressure ratio and ballistic efficiency of the accelerator are evaluated and their maximum values are 0.032 and 0.068, respectively. The code indicates possibility of achieving high velocity of 7 km/s on utilising gaseous mixture of  $2H_2 + O_2$  in the operation. Velocity range suitable for operation of the accelerator lies between 3.8 - 7.0 km/s. Maximum thrust value is 33721 N which corresponds to the projectile velocity of 5 km/s.

### NOMENCLATURE

$u$	Flow velocity	$M^*$	Non-dimensional resultant velocity of the flow over the cone
$\bar{u}, \bar{v}$	Velocity components of flow over the cone	$\alpha$	Angle of discrete expansion wave with the horizontal
$\bar{u}^*, \bar{v}^*$	Non-dimensional velocity components	$\nu$	Prandtl-Mayer angle
$\bar{m}$	Mass flow rate	$R$	Tube radius
$m$	Molecular weight	$R_p$	Projectile radius
$F$	Thrust	$A$	Cross-sectional area of flow
$p$	Pressure	$A_p$	Projectile cross-sectional area
$P$	Stagnation pressure	$L_p$	Projectile length
$t$	Static temperature	$C_p$	Specific heat at constant pressure
$T$	Stagnation temperature	$R''$	Gas constant
$M$	Mach number	$H$	Height of intersection of waves from the projectile surface

$D.T$	Ignition delay time
$A.E$	Activation energy
$a$	Local speed of sound
$a^*$	Critical speed of sound
$\delta p$	Projectile half-cone angle
$\delta$	Angle of flow with the horizontal
$\varepsilon$	Wave angle
$\psi$	Arbitrary angle between $\delta$ and $\varepsilon$
$\gamma$	Ratio of specific heats
$\rho$	Density
$\delta q$	Heat of combustion
s0-s10	Flow streamlines
$\lambda$	Constant coefficient in thermal explosion theory
$\beta$	Angle of flow velocity with the streamline
<i>Subscripts &amp; superscripts</i>	
1 to 15	Regions of flow field
2, 3	Region between conical shock and projectile cone
$rr$	Reactants
$pr$	Products
'	Before shock reflection
"	Before expansion wave

## 1. INTRODUCTION

Ram accelerator is a ramjet-in-tube device conceived to accelerate the projectile to very high velocity by chemical means. Velocity of 2.2 km/s is reported to have been experimentally obtained. There exist number of modes of its operation like thermally-choked and detonation modes which span the velocity range of 0.7-12.0 km/s. These modes differ from each other in the manner the combustion of gases takes place in them. For example, combustion in thermally-choked type with velocity range of 0.7-3.0 km/s is caused by an onboard ignitor. Limiting velocity of the projectile in this mode is the C-J detonation velocity of the mixture. On the other hand, combustion in detonation type mode is triggered by self-ignition of the gases where starting or entry velocity of the projectile in the accelerator tube itself can be higher than the C-J detonation velocity of the gaseous mixture. Limiting velocity in this mode, where ballistic parameters approach zero, is very high and is of the order of

8-12 km/s depending upon the type of gaseous mixture used in the operation.

The objective of the paper is to present the methodology of analysing the detonation type ram accelerator followed by computation of flow properties in all critical regions of the flow field. Ballistic parameters like thrust-pressure ratio and ballistic efficiency are determined in order to estimate overall performance potential of the device. Mathematical modelling of all major flow processes taking place during the operation of the accelerator is explained. Gaseous mixture chosen for the analysis is  $2H_2 + O_2$ .

## 2. OPERATION

Gaseous mixture is filled at high pressure in the accelerator tube using a suitable tube-end closure device to hold the mixture. The projectile is forced into the tube with the velocity higher than the detonation velocity of the mixture. Launch scenario involves initial acceleration of the projectile by a gas gun followed by entry of the projectile in the accelerator (Fig. 1). Initiation of a conical shock wave from the concave corner at the projectile tip and its subsequent reflection from the tube wall raises the pressure and the temperature of the mixture which is sufficient for its self-ignition. Shock ignition of gases raises the pressure and temperature of the gases. High pressure product gases expand continuously rearward, thereby generating thrust which accelerates the projectile. Since the combustion zone is very near to the reflected shock, combination of reflected shock and combustion zone is termed as detonation front. As the reflected shock is oblique in orientation, therefore such type of ram accelerators are also called oblique detonation ram accelerators.

## 3. MODELLING

Flow field is assumed to be in steady-state motion wrt the stationary projectile. Control volume is indicated by dashed lines marking the projectile tip and end of gaseous expansion. For computation purpose, control volume is divided in regions (1 to 15) of interest. Modelling assumptions are:

- Accelerator tube is frictionless.
- Effect of boundary layer between the projectile

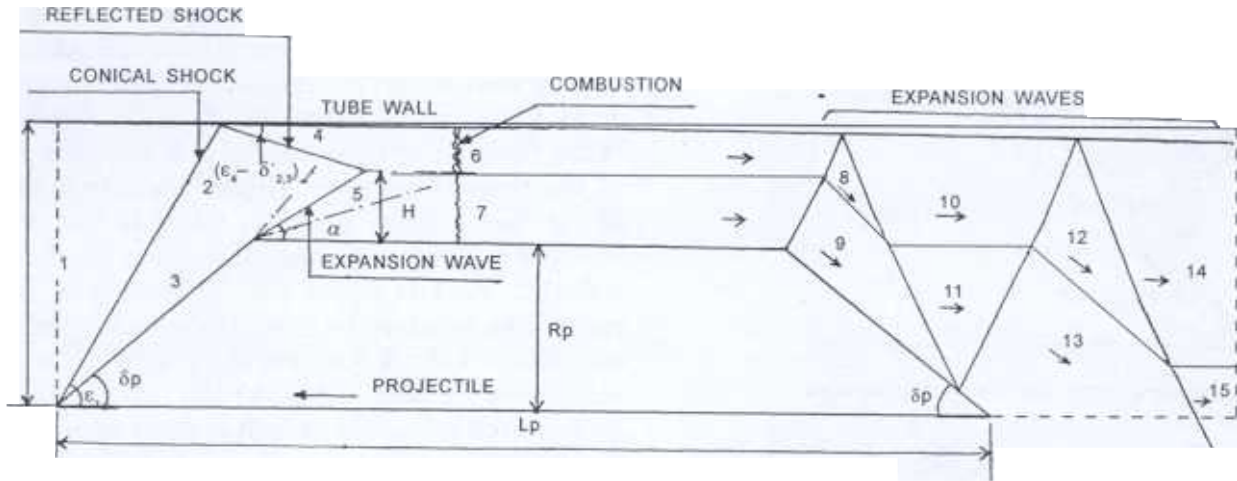


Figure Flow processes in detonation type ram accelerator

surface and gases is ignored.

- (c) Radiational effects and dissociation of combustion products are not considered.

Gaseous thrust responsible for acceleration of the projectile is given by

$$F = \{p_{14} \cdot A_{14} + p_{15} (A_1 - A_{14}) - p_1 \cdot A_1\} + \{\bar{m}_{14} u_{14} + \bar{m}_{15} \cdot u_{15} - (\bar{m}_{14} + \bar{m}_{15}) \cdot u_1\}$$

where

$$\bar{m}_{14} = \bar{m}_4, \bar{m}_{15} = \bar{m}_5 \text{ and } \bar{m}_4 + \bar{m}_5 = \bar{m}$$

#### 4. METHODOLOGY & ANALYSIS

High speed movement of the projectile in the tube forces the gases to flow over the nose cone of the projectile, thereby forming a conical shock wave. Governing differential equations for Taylor-Maccoll supersonic, axisymmetric and irrotational conical flow<sup>1</sup> over the projectile given in Appendix 1 as Eqns (7) and (8) enable to determine the flow parameters in the entire region between 2 and 3. Starting value of wave angle ( $\epsilon_1$ ) is taken as  $\delta p + 1/2 [\sin^{-1} (1/M_1)]$  and all the flow parameters immediately behind the conical shock wave in region 2 are obtained by oblique shock relationships given by Eqns (1) to (6). Non-dimensional velocity components obtained in region 2 initialise for Eqns (7) and (8) which are solved by Runge-Kutta numerical method with a suitable step size of  $\psi$

(Fig. 2). Region from 2 to 3 is divided into ten streamlines and integration is continued up to the cone surface. As need arises, the wave angle is modified till the boundary condition ( $\bar{v}^* = 0$ ) is satisfied at the cone surface as the flow at the projectile surface has only a single component along the surface and zero normal component. Since the flow is irrotational in the region between 2 and 3, conditions of constant stagnation pressure and stagnation density along with the equation of state enable to determine the flow parameters anywhere in the flow field. Variation of Mach number across the streamlines is observed not to be significantly large. Therefore, average values of the flow parameters are considered to make the process suitable for subsequent computation. This is done by replacing all the ten flow streamlines by two uniform streamlines. One represents the state of flow before shock reflection and the other the state of flow before flow expansion, in such a manner that sum of mass flow rates evaluated after reflection and expansion matches with the initial mass flow in region 1 (Fig. 1). Conical shock wave on striking the tube wall gets reflected as another shock wave to satisfy the solid wall boundary condition. Flow parameters behind the reflected shock wave in region 4 are computed by wave angle theory for flows over the wedge<sup>2</sup>. For the known Mach number of the flow  $M'_{2,3}$  and turning angle of  $\delta'_{2,3}$ , wave angle  $\epsilon_4$ , is obtained from wave angle charts for oblique shocks. On

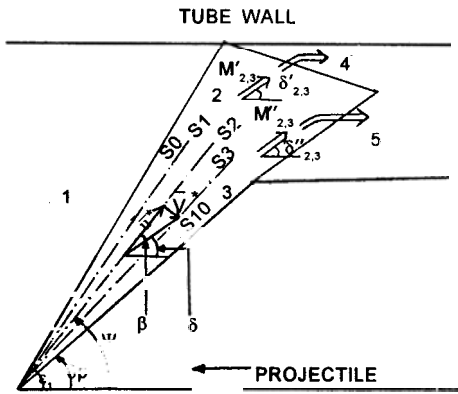


Figure 2. Flow over the projectile cone

defining  $\hat{M}_{2,3}$  as in Eqn (9),  $\hat{M}_4$  corresponding to  $\hat{M}_{2,3}$  is obtained from normal shock tables. Equation (10) determines the Mach number  $M_4$  in region 4. Other flow parameters are obtained from Eqns (1) to (3) using wave angle  $\varepsilon_4$ , state 1 of the equation corresponding to Taylor-Maccoll flow before reflection in region 2-3 and state 2 corresponding to region 4.

Supersonic flow of the gases over the projectile front convex shoulder leads to emanation of an expansion fan. Expansion fan is replaced by the discrete wave and Prandtl-Mayer analysis<sup>2</sup> for uniform flow is adopted for modelling the expansion process followed by determination of the flow properties in region 5. Prandtl-Mayer angle  $\nu''_{2,3}$  corresponding to Mach number  $M''_{2,3}$  is found out. New value of Prandtl-Mayer angle in region 5 is obtained from Eqn (11) and corresponding Mach number  $M_5$  is read from data tables. Stagnation temperature and pressure before and after expansion is the same which leads to evaluation of the remaining flow parameters in region 5. Origination of expansion wave limits the extent of reflection of the conical shock wave and so neutralise each other. The purpose of these two is to render the flow parallel to the tube wall in fulfillment of physical requirement of the flow. Equation (12) helps to obtain the intersection point of two waves which in turn determines the area and mass flow rates in regions 4 and 5 as indicated by Eqn (13).

Exothermic reaction of gaseous mixture of fuel and oxidiser causes the temperature of the mixture to rise. This self-acceleration process proceeds slowly

at first until after some finite delay time, the system explodes or detonates. A mixture of equilibrium products is formed at the temperature and pressure that are much higher than the initial values. Ignition delay for adiabatic explosion given by Eqn (14) is the function of temperature and required A.E of the gaseous mixture<sup>3</sup>. Higher the temperature of the fuel oxidiser mixture, lesser is the delay time for explosion. Temperature jump across the reflected shock in region 4 is sufficiently large to cause a short delay to thermal explosion behind the reflected shock whereas the concurrent delay behind the incident conical shock is quite large<sup>4</sup>. Body of the projectile is kept long to ensure that the detonation wave originates at the body before the rear shoulder.

Effect of heat addition is to decelerate the flow. Two arbitrary values of temperature in region 6 are assumed. Because of nonavailability of the value of specific heat of the product gas ( $H_2O$ ) at high temperature and pressure in JANAF thermochemical data tables—therefore in each case, the value of specific heat at constant pressure is approximated from the polynomial correlating specific heat with temperature<sup>2</sup>. Two output temperature values are obtained from Eqns (15) and (16) by determining Mach number of the product gas in each iteration from Rayleigh line equation<sup>2</sup>. Heat of combustion value corresponds to state 4. Final temperature of the gases after detonation is obtained by numerical (secant) method<sup>2</sup>. Specific heat is once again calculated corresponding to final temperature and one more iteration is repeated to obtain the final Mach number of the product gas. Other flow parameters are found out by Eqns (17) to (19) representing equations of conservation of mass and equation of state. Heat released in the detonation zone ignites the mixture down below in region 5. Combustion modelling already explained holds good in this case also except that heat of combustion now corresponds to state 5. Flow in regions 6 and 7 are considered separately for subsequent expansion process.

Expansion wave generated at the rear convex shoulder of the projectile is reflected from the tube wall to fulfill the physical requirement of the flow to maintain its direction parallel to the tube wall. The process gets repeated when the reflected

wave strikes the projectile. The technique explained earlier for analysing the expansion waves is again used and flow parameters up to regions 14 and 15 are computed. Flow areas in regions after expansion are determined by conservation of mass relationship.

## 5. RESULTS & DISCUSSION

Conventional configuration of the projectile is chosen and its parameters are selected in such a manner that the combustion occurs behind the front shoulder of the projectile. A computer code based

Table 1. Flow properties for Taylor-Maccoll flow with  $\epsilon_1 = 16.5247^\circ$

Streamline	$\psi$ (deg.)	$\delta$ (deg.)	$\bar{u}^*$	$\bar{v}^*$	$M^*$	$M$
s0 (region 2)		11.6780	2.28300	-0.1934	2.2915	5.9220
s1		11.9120	2.28420	-0.1740	2.2908	5.9060
s2		12.1400	2.28490	-0.1548	2.2901	5.8930
s3		12.3600	2.28550	-0.1357	2.2896	5.8810
s4		12.5900	2.28610	-0.1166	2.2891	5.8710
s5		12.8100	2.28660	-0.0975	2.2886	5.8620
s6		13.0450	2.28690	-0.0784	2.2883	5.8550
s7		13.2700	2.28720	-0.0590	2.2880	5.8500
s8		13.5100	2.28750	-0.0390	2.2878	5.8460
s9		13.7500	2.28764	-0.0190	2.2877	5.8430
s10 (region 3)		14.0002	2.28769	0.0000	2.2876	5.8429

$\delta p = 14^\circ$ ,  $Rp = 1.29$  cm,  $Lp = 14.7$  cm,  $R = 1.5$  cm,  $A_1 = 7.06$  cm<sup>2</sup>

Average values considered for subsequent analysis:  $M'_{2,3} = 5.9$ ,  $\delta'_{2,3} = 11.91^\circ$ ,  $M''_{2,3} = 5.86$ ,  $\delta''_{2,3} = 13.18^\circ$

Table 2. Values of flow parameters of the reactants around the projectile in regions of the flow field prior to detonation at projectile velocity of 5000 m/s

Regions	1	2	3	4	5
$p$ (atms)	100.0	799.50	868.30	3617.30	97.73
$t$ (K)	298.0	680.90	697.10	1164.32	373.40
$\rho$ ( kg/m <sup>3</sup> )	48.4	169.40	179.70	448.20	37.75
$u$ (m/s)	5000.0	4810.00	4802.00	4534.00	4963.00
$M$	9.3	5.92	5.84	4.27	8.25

Reactants:  $2H_2 + O_2$

$\epsilon_1 = 16.5247^\circ$ ,  $\epsilon_4 = 19.7^\circ$ ,  $\alpha = 13.726^\circ$ ,  $H = 0.1242$  cm

$cp_1 = 2389$  J/kg.K,  $m_{pr} = 12.01$ ,  $R''_{pr} = 692.2$  J/kg.K,  $\gamma_1 \cong 1.4$

Table 3. Values of flow parameters of the products around the projectile in regions of the flow field ahead of detonation front at projectile velocity of 5000 m/s

Regions	6	7	8	9	10	11	12	13	14	15
	20543.00	1564.00	11354.00	807.00	5066.00	413.00	2819.00	167.00	1134.00	66.60
	6496.00	6141.00	5994.00	5611.00	5373.00	5120.00	4963.00	4527.00	4387.00	3991.00
	682.00	54.90	408.00	31.00	203.00	17.40	122.00	7.90	55.81	3.50
	2980.00	3407.00	3507.00	3898.00	4066.00	4303.00	4397.00	4746.00	4823.00	5114.00
	1.60	1.88	1.96	2.25	2.40	2.60	2.70	3.05	3.15	3.50

Product:  $H_2O$

$cp_6 = 3409$  J/kg.K,  $cp_7 = 3383$  J/kg.K,  $m_{pr} = 18$ ,  $R''_{pr} = 461.9$  J/kg.K,  $\gamma_6 \cong 1.156$ ,  $\gamma_7 \cong 1.158$

$\delta q_4 \cong 2.48 \times 10^5$  J/mol,  $\delta q_5 \cong 2.42 \times 10^5$  J/mol,  $A_{10} = 1.93$  cm<sup>2</sup>,  $A_{11} = 2.65$  cm<sup>2</sup>,  $A_{14} = 5.93$  cm<sup>2</sup>

on previously mentioned equations is formulated to estimate the performance parameters of the accelerator. The code is run at the three projectile velocities of 4 km/s, 5 km/s and 7 km/s. Table 1 presents the projectile data and typical flow properties for Taylor-Maccoll flow corresponding to the instant when the projectile moves at 5000 m/s in the gaseous mixture of  $2H_2 + O_2$  filled at 100 atms. in the tube. Mixture possesses the acoustic speed of 537 m/s. Tables 2 and 3 highlight the sample values of flow parameters in different regions of the control volume for the same configuration. It is necessary to emphasise that they denote the average values over the cross-section of the flow. Maximum values of thrust-pressure ratio defined by  $\{F / (p_6 \times Ap)\}$  and ballistic efficiency defined by  $\{(F \times u_1) / (\bar{m}_4 + \bar{m}_5) \cdot \delta q\}$

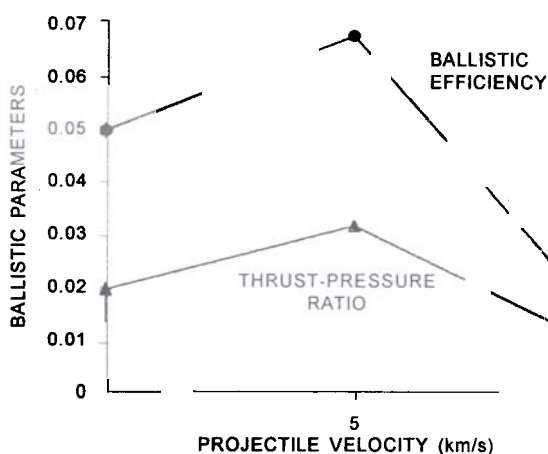


Figure 3. Variation of ballistic parameters with projectile velocity.

are 0.032 and 0.068, respectively with thrust value of 33721N. Variation in these ratios with change in projectile velocity is plotted in Fig. 3.

Below projectile velocity of 3.8 km/s, temperature after the shock reflections is low enough. Delay time for explosion is too large and therefore detonation wave does not form at the projectile body<sup>4</sup> leading to zero thrust. For projectile velocity at and above 3.8 km/s, reflected shock wave strikes the nose cone of the projectile which causes origination of one more oblique shock. Since the flow is turbulent as high Reynolds number confirms, shock reflection from the projectile surface is treated as regular reflection with remote chances of flow separation<sup>5</sup>.

Auto-ignition takes place after the reflection of the second shock wave<sup>4</sup>. Pressure, temperature and density values of the mixture after final reflection in region.4 are high with reduced Mach number because of more shock waves the flow has to encounter. Equation (19) indicates dependance of pressure value after combustion on the state of flow before combustion in region 4. Pressure of the product gases in region 6 is therefore less which results in low thrust. With increase in projectile velocity and the starting Mach number, wave angles of oblique shocks reduce which results in reduced drop in velocity across the shock waves and therefore increased gas velocities and relatively lesser increase in temperature and density of the mixture up to region 4. Jump in temperature and density across detonation wave keeps on increasing leading to higher pressure values in region 6 after combustion. Maximum thrust is attained at 5 km/s where ignition occurs by first reflection of the conical shock wave as shown in Fig. 1. Beyond 5 km/s, ballistic parameters drop. Heat of combustion does not increase significantly with increasing temperature and pressure. The ratio of heat of combustion and dynamic energy of the gaseous mixture at entry point in region 1 of the control volume therefore consistently reduces which limits the operation of the accelerator at 7 km/s. Above 7 km/s, initial conical shock wave strength is sufficient to ignite the mixture prematurely in the region 2 to 3 thereby subjecting the nose cone of the projectile to high pressure and consequently resulting in negative thrust<sup>4</sup>.

## 6. NEW CONCEPTS

Minimum starting operational velocity of the projectile in the case discussed is 3.8 km/s which itself is very high and calls for a separate system like a gas gun to achieve it. The problem is overcome to some extent by modifying the design of the projectile which helps in reducing the entry velocity of the projectile much below the detonation velocity of the gaseous mixture. Front convex shoulder of the projectile configuration already explained is replaced by a concave ramp which gives rise to one more shock wave instead of expansion wave<sup>6</sup>. In the absence of expansion wave, reflected shock waves continue uninterrupted up to the projectile

further reduces the Reynolds number. Reflected shock wave on striking the boundary layer adjacent to the projectile body forces its separation. Phenomenon of separation is more predominant in laminar boundary layers<sup>5</sup>. Separation leads to increase in temperature and pressure in the boundary layer which triggers ignition. Since the extent of combustion in a thin boundary layer is quite low, thrust value is initially negative which causes a temporary fall in the projectile velocity. But as detonation velocity of the mixture is much higher than the projectile velocity, combustion wave gradually spreads forwards and upwards, towards the tube wall encompassing more area of flow and maintaining a single detonation front in contrast to the case discussed earlier where new detonation fronts are continuously formed. Thrust value consequently increases from negative to positive value leading to increased projectile velocity. Unstart condition is reached when the combustion front moves up to the nose cone of the projectile resulting in reduced thrust.

Starting projectile velocity in this case can be as low as 2136 m/s in the hydrogen-oxygen-argon mixture which is achievable by thermally-choked ram accelerator<sup>6</sup>. Any further reduction possible in starting velocity should interestingly enable direct launching of the projectile by conventional techniques. But penetration aspect of such a typical and unconventional projectile shape calls for investigation. However, if ram accelerators are found suitable only for space applications, then all those aspects governing projectile penetration at target end will not be important at all.

## 7. CONCLUSION & FUTURE SCOPE

Mathematical model presented indicates possibility of achieving projectile velocity up to 7 km/s in oblique detonation ram accelerator using conventional projectile design. Same procedure can be applied to investigate performance of the accelerator using other types of gaseous mixtures with higher acoustic speeds and different heats of combustion.

Influence of temperature on the specific heats and their ratio for both reactants as well as products is ignored in the analysis. For example, the ratio of specific heats of the reactants in region 4 is

found to have reduced from 1.40 to 1.33. This effect can be considered in all the regions of the control volume although overall change in the thrust value may not be very significant. Effect of variation in Mach number of the streamlines across the Taylor-Maccoll flow can be included by dividing the flow region into larger number of streamlines and independently analysing all of them throughout the control volume. Consideration of non-uniform flow before shock reflection and the expansion wave will lead to formation of series of moderate expansions and reflections all over the body of the projectile. Inclusion of all this however calls for enormous computation.

Accuracy of the results can further be enhanced by incorporating radiational effects due to high temperature of the gases and skin friction between the projectile and the gases. Time delay for auto-ignition can also be evaluated by finding out the necessary parameters like activation energy and constant coefficients as indicated in Eqn (14). Determination of critical pressure and temperature will enable to model thermal explosion with heat losses.

## ACKNOWLEDGEMENTS

The author is thankful to Sh R. Bhattacharya, Scientist F, Armament Research & Development Establishment, Pune, for providing necessary support during the work and to Dr S.K. Salwan, Director, of the Establishment for allowing him to pursue the subject.

## REFERENCES

1. Zucrow, M.J. & Hoffman, J.D. *In Gas dynamics*, Vol. II. John Wiley & Sons, pp. 169-76.
2. Zucrow, M.J. & Hoffman, J.D. *In Gas dynamics*, Vol. I. John Wiley & Sons, p.387.
3. Strehlow, R.A. *Combustion fundamentals*. McGraw-Hill Book Company, USA, 1984. pp.172-79.
4. Brackett, D.C. & Bogdanoff, D.W. Computational investigation of oblique detonation ramjet-in-tube concepts. *Journal of Propulsion*, May-June 1989, 5, 276-81.

- 4 Brackett, D.C. & Bogdanoff, D.W. Computational investigation of oblique detonation ramjet-in-tube concepts. *Journal of Propulsion*, May-June 1989, 5, 276-81.
- 5 Shapiro, A.H. The dynamics and thermodynamics of compressible fluid flow, Vol. II. 1141p.
- 6 Yungster, S.; Radakrishnan, K. & Rabinowiz, M.J. Reacting flow establishment in ram accelerators: A numerical study. *J. Propul. Power*, 1998, 14(1), 14.

**Contributor**



**Shri Sunil Bhat** obtained his ME (Mechanical) securing 1st position from University of Poona, Pune, in 1997. He joined DRDO at the Armament Research & Development Establishment, Pune, in 1991. Presently, he is working as Senior Scientist. His area of research includes: development of multibarrel rocket launcher system.



**1. Conical Shock Relations**

$$\frac{p_2}{p_1} = \frac{2\gamma_1}{\gamma_1 + 1} \left[ M_1^2 \sin^2 \varepsilon_1 - \frac{\gamma_1 - 1}{2\gamma_1} \right]$$

$$\left. \frac{\rho_1}{\rho_2} = \frac{\tan \beta}{\tan \varepsilon_1} = \frac{2}{\gamma_1 + 1} \right]$$

$$\frac{t_2}{t_1} = \frac{p_2 \cdot \rho_1}{p_1 \cdot \rho_2} \quad (3)$$

$$\frac{M_2^*}{M_1^*} = \frac{\sin \varepsilon_1}{\sin \beta} \left[ \frac{2}{(\gamma_1 + 1) M_1^2 \sin^2 \varepsilon_1} + \frac{\gamma_1 - 1}{\gamma_1 + 1} \right] \quad (4)$$

where

$$M_1^* = \left[ \frac{(\gamma_1 + 1) M_1^2}{2 + (\gamma_1 - 1) M_1^2} \right]^{1/2}$$

$$\bar{u}_2^* = M_2^* \cos \beta$$

$$\bar{v}_2^* = -M_2^* \sin \beta \quad (6)$$

**2. Generalised Taylor-Maccoll Flow Equations**

$$\frac{d\bar{u}^*}{d\psi} = \bar{v} \quad (7)$$

$$\frac{d\bar{v}^*}{d\psi} = -\bar{u}^* + \frac{\left\{ \frac{a}{a^*} \right\}^2 \{ \bar{u}^* + \bar{v}^* \cot \psi \}}{(\bar{v}^*)^2 - \left\{ \frac{a}{a^*} \right\}^2}$$

where

$$\bar{u}^* = \frac{\bar{u}}{a^*}, \bar{v}^* = \frac{\bar{v}}{a^*},$$

$$\left\{ \frac{a}{a^*} \right\}^2 = \frac{\gamma_1 + 1}{2} - \frac{\gamma_1 - 1}{2} M_1^2,$$

$$M^* = \sqrt{\bar{u}^{*2} + \bar{v}^{*2}}$$

**3. Reflected Shock Wave**

$$\hat{M}_{2,3} = M'_{2,3} \sin \varepsilon_4 \quad (9)$$

$$M_4 = \frac{M_4}{\sin(\varepsilon_4 - \delta'_{2,3})} \quad (10)$$

**4. Expansion Wave**

$$v_5 = v''_{2,3} + \delta''_{2,3} \quad (11)$$

$$P_5 = P_{2,3}, T_5 = T_2$$

**5. Intersection of Expansion & Reflected Wave**

$$H = \frac{R - Rp - \left[ \frac{Rp}{\tan \delta p} - \frac{R}{\tan \varepsilon_1} \right] \tan(\varepsilon_4 - \delta'_{2,3})}{\tan(\varepsilon_4 - \delta'_{2,3}) + \frac{\tan \alpha}{\tan \alpha}} \quad (12)$$

$$\bar{m}_4 = \rho_4 \cdot A_4 \cdot u_4 \quad \text{and} \quad \bar{m}_5 = \rho_5 \cdot A_5 \cdot u_5 \quad (13)$$

**6. Ignition Delay for Adiabatic Explosion**

$$D.T = \frac{R''_4 t_4^2}{(A.E) \lambda} \exp \left[ \frac{A.E}{R''_4 t_4} \right] \quad (14)$$

**7. Supersonic Combustion**

$$cp_6 T_6 = cp_1 T_1 + \delta q \quad (15)$$

$$cp_1 T_1 + \delta q = cp_6 t_6 \left( 1 + \frac{\gamma_6 - 1}{2} M_6^2 \right) \quad (16)$$

$$u_6 = M_6 (\gamma_6 R''_6 t_6)^{1/2} \quad (17)$$

$$\rho_6 = \frac{\bar{m}_6}{A_6 \cdot u_6} \quad \text{where} \quad \bar{m}_6 = \bar{m}_4 \quad (18)$$

$$\frac{p_6}{p_4} = \frac{\rho_6 R''_6 t_6}{\rho_4 R''_4 t_4}$$

where

$$R''_6 = \frac{R''(\text{universal})}{m_{pr}} \quad \text{and} \quad R''_4 = \frac{R''(\text{universal})}{m_{rr}} \quad (19)$$